Available online at www.sciencedirect.com
SCIENCE DIRECT
Thermochimica Acta 446 (2006) 121–127
thermochimica acta
www.elsevier.com/locate/tca

Crystal growth kinetics in $(GeS_2)_{0.2}(Sb_2S_3)_{0.8}$ glass

Daniel Švadlák [a,*], Pavla Pustková [b], Petr Koštál [a], Jiří Málek [a]

[a] *Department of Physical Chemistry, University of Pardubice, Cs. Legii 565, Pardubice 53210, Czech Republic*
[b] *Department of Inorganic Technology, University of Pardubice, Cs. Legii 565, Pardubice 53210, Czech Republic*

Abstract

The crystal growth kinetics of Sb_2S_3 in $(GeS_2)_{0.2}(Sb_2S_3)_{0.8}$ glass has been studied by DSC and optical microscopy. The linear growth kinetics of Sb_2S_3 has been observed in the temperature range $525\,K \leq T \leq 556\,K$ ($E_G = 295 \pm 3\,kJ\,mol^{-1}$). From the reduced growth rate plot (i.e., growth rate corrected for viscosity) as a function of supercooling it has been found that the most probable mechanism is interface controlled 2D nucleated growth. The DSC data, corresponding to the bulk sample under isothermal and non-isothermal, can be described by the Johnson–Mehl–Avrami equation for the kinetic exponent $m \cong 2$.

Keywords: Crystal growth; Crystallization kinetics; Growth rate; Viscosity; Chalcogenide glass; Nucleation-growth model

1. Introduction

Antimony trisulphide (stibnite) is an important semiconductor in view of its photosensitive and thermoelectric properties [1]. It is used in television cameras, microwave devices and various optoelectronic devices [2,3]. Sb_2S_3 thin films can also be used for write-once-read-manytimes (WORM) type optical storage applications [4].

In this paper we attempt to show a direct connection between our measurements of crystals growth (studied by optical microscopy) and viscosity and DSC data of crystallization kinetics in glassy $(GeS_2)_{0.2}(Sb_2S_3)_{0.8}$ published recently [5]. Only through viscous flow of undercooled melts it seems to be effective to completely describe crystallization behavior likewise was described in papers by Málek et al. [6,7].

2. Experimental

The bulk glassy samples were prepared by direct synthesis from germanium, antimony (purity 99.999%) and three times distilled sulphur in evacuated fused silica ampoules (inside diameter 16 mm and length 140 mm). Total charge was 12 g. The ampoule was evacuated to a pressure 10^{-3} Pa for 30 min and sealed. Then it was placed in a rocking furnace. After synthesis and homogenization (20 h, $T = 1223$ K) the melt was quenched in ice water. The amorphous character was confirmed by X-ray diffraction (XRD). Optical microscopy was used to verify homogeneity of prepared materials.

The samples were prepared as a bulk specimen polished to optical quality. They were about 3 mm × 4 mm in size and 1.5 mm thick. These prepared samples were heated in a computer-controlled furnace at selected temperatures (525–556 K) for various times. The dominantly growing proportion of the observed crystals was studied by optical microscopy. The optical microscope Olympus BX60 with reflect light mode was used. The sizable difference in reflectivity between the amorphous glassy matrix and the crystalline phase enables the observation of crystal growth.

The calorimetric experiments were performed by a Perkin-Elmer differential scanning calorimeter Pyris 1 (calibrated with standards Hg, Ga, In, Sn, Pb and Zn). The bulk samples (about 30 mg) of the studied glass were prepared in the form of thin plates both-side polished to optical quality. They were measured in the standard aluminum sample pans. All measurements were done under dry nitrogen atmosphere. The crystallization behavior was studied under isothermal (589–601 K) and non-isothermal conditions (323–673 K, heating rates 5–30 K min^{-1}). Heating rate 200 K min^{-1} was used to heat samples to temperature selected for isothermal crystallization measurements.

XRD analysis of amorphous and crystallized sample was performed using a Bruker AXS X-ray diffractometer D8 Advance equipped by scintillation counter, utilizing Cu Kα radiation (40 kV, 30 mA). The scans were taken over the scattering angles 2θ from 5 to 65° at the scanning speed of 0.12° min^{-1}.

* Corresponding author.
E-mail address: daniel.svadlak@upce.cz (D. Švadlák).

0040-6031/$ – see front matter © 2006 Elsevier B.V. All rights reserved.
doi:10.1016/j.tca.2006.05.013

The samples were analyzed by an electron scanning microscope JEOL JSM-5500LV and by electron-dispersive X-ray analyzer IXRF Systems (detector GRESHAM Sirius 10). The accelerating voltage of the primary electron beam was 20 kV. The quantitative analysis was performed by using the standards purchased from C.M. Taylor Corporation, USA.

Viscous behavior of $(GeS_2)_{0.2}(Sb_2S_3)_{0.8}$ undercooled melt in the range of 10^7–10^{13} Pa s was studied by penetration viscosimetry using the thermomechanical analyzer TMA CX03R (R.M.I., Czech Republic). The power in the range of 10–500 mN was applied on the hemispherical indenter which was penetrated into the sample under isothermal conditions. Duration of these isothermal measurements was between 0.5 and 50 h (corresponds to 549 and 483 K). Other details of the used method and instrument are described elsewhere [8].

3. Results

3.1. DSC measurements of crystallization kinetics

This part of paper deals with crystallization kinetics of Sb_2S_3 measured by DSC method in glassy $(GeS_2)_{0.2}(Sb_2S_3)_{0.8}$ bulk. The crystallization behavior was observed under non-isothermal and isothermal conditions. In the temperature range 323–673 K was determined the glass transition temperature T_g (about 510 K at heating rate 10 K min^{-1}) and one exothermal crystallization peak. This exothermal peak was found in temperature range 582–666 K for non-isothermal conditions at heating rates 5–30 K min^{-1} (Fig. 1) and in temperature range 589–601 K for isothermal conditions (Fig. 2). These isothermal temperatures represent an optimum condition for isothermal measurement. At higher temperatures the crystallization response is too fast and due to significant time constant of the DSC instrument some part of experimental data may be lost. Lower temperatures bring another difficulty because the signal-to-noise ratio

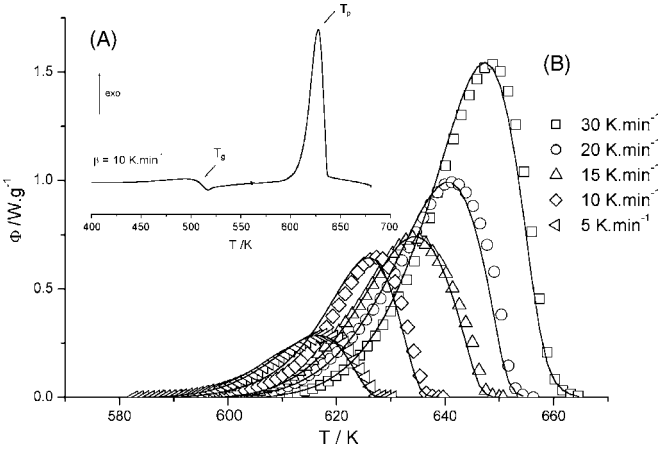

Fig. 1. (A) Typical non-isothermal DSC curve over all the temperature range of bulk sample $(GeS_2)_{0.2}(Sb_2S_3)_{0.8}$ for heating rate 10 K min^{-1} (T_g is the glass transition temperature, T_p is the temperature of the maximum of crystallization peak). (B) Non-isothermal DSC curves for crystallization of Sb_2S_3 in $(GeS_2)_{0.2}(Sb_2S_3)_{0.8}$ bulk sample for different heating rates (points). The solid lines were calculated using Eqs. (5) and (6) for $E = 180$ kJ mol^{-1}, $m = 2$ and $\ln(A/s^{-1}) = 30.0 \pm 0.1$.

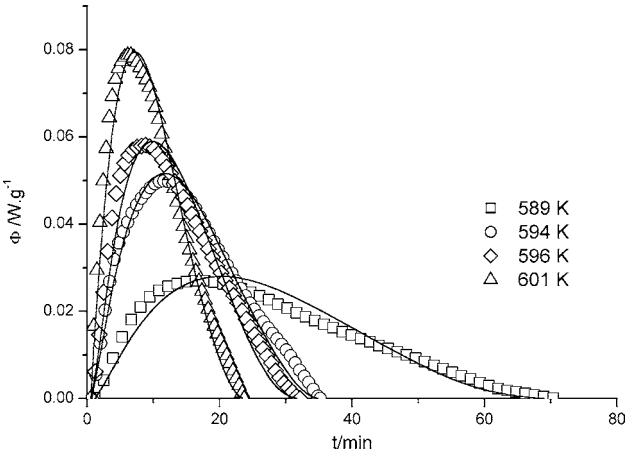

Fig. 2. Isothermal DSC curves for crystallization of Sb_2S_3 in $(GeS_2)_{0.2}(Sb_2S_3)_{0.8}$ bulk samples (points). The solid lines were calculated using Eqs. (5) and (6) for $E = 268$ kJ mol^{-1}, $m = 2$ and $\ln(A/s^{-1}) = 47.2 \pm 0.1$.

negatively affects the accuracy of the measurement. The crystallization enthalpy corresponding to the area under exothermic peaks was found to be -65 ± 2 J g^{-1} for non-isothermal conditions and -60 ± 1 J g^{-1} for isothermal conditions.

The samples were analyzed by X-ray diffraction (Fig. 3) before and after DSC measurements. The crystallization product was identified as the orthorhombic form of Sb_2S_3 (stibnite).

Next important kinetic parameter is the apparent activation energy. From data measured under non-isothermal conditions

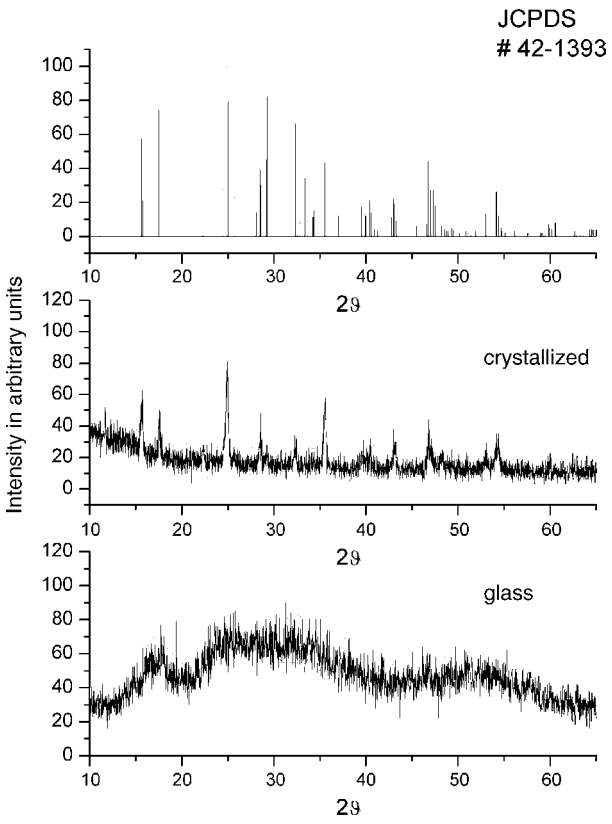

Fig. 3. X-ray diffraction pattern of prepared glass and crystallized material. The bar diagram corresponds to the JCPDS file of crystalline Sb_2S_3 (stibnite).

we calculated the value of this activation energy using Kissinger method [9]:

$$\ln\left(\frac{\beta}{T_p^2}\right) = \text{const} - \frac{E}{R} \times \left(\frac{1}{T_p}\right) \quad (1)$$

where β is the heating rate, T_p is the temperature of the maximum of crystallization peak, E is the apparent activation energy. Dependence of $\ln(\beta/T_p^2)$ on $1/T_p$ is the straight line with slope $180 \pm 4\,\text{kJ mol}^{-1}$.

The other method for non-isothermal conditions is isoconversional method [10]. This method can be used in equivalent form also for isothermal conditions.

$$\ln \Phi_\alpha = \ln[(\Delta H \times A \times f(\alpha))] - \frac{E}{R} \times \frac{1}{T_\alpha} \quad (2)$$

where Φ is the heat flow, ΔH is the crystallization enthalpy, A is the pre-exponential factor, $f(\alpha)$ is the analytical expression of the kinetic model, α is the conversion ratio and E is the apparent activation energy.

The plots of $\ln \Phi_\alpha$ versus $1/T_\alpha$ with straight lines for different values of α were obtained. From these slopes were calculated the values of apparent activation energy. The average value of this energy calculated in the range $0.2 \leq \alpha \leq 0.6$ is $268 \pm 40\,\text{kJ mol}^{-1}$ for isothermal conditions and $180 \pm 4\,\text{kJ mol}^{-1}$ for non-isothermal conditions.

3.2. Viscosity measurements of $(GeS_2)_{0.2}(Sb_2S_3)_{0.8}$

The viscous behavior of $(GeS_2)_{0.2}(Sb_2S_3)_{0.8}$ was studied by penetration viscometry in the range of 10^7–10^{13} Pa s. Obtained temperature dependence of viscosity is shown in Fig. 4. We calculated the apparent activation energy E_η of viscous flow from Arrhenius plot (3):

$$\eta = \eta_0 \exp\frac{E_\eta}{RT} \quad (3)$$

where T is the temperature, η is the measured viscosity and η_0 is a constant. This activation energy E_η is $439 \pm 6\,\text{kJ mol}^{-1}$ and temperature corresponding to viscosity 10^{12} Pa s is 494 K.

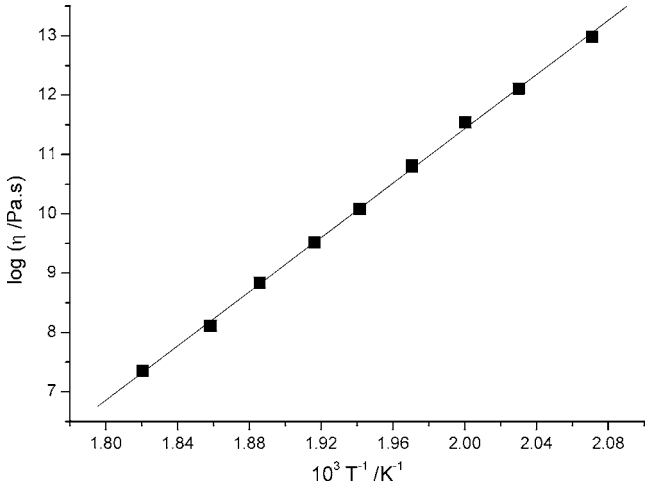

Fig. 4. Temperature dependence of viscosity of $(GeS_2)_{0.2}(Sb_2S_3)_{0.8}$ undercooled melt.

3.3. Optical measurements of crystal growth in bulk $(GeS_2)_{0.2}(Sb_2S_3)_{0.8}$ composition

Only one type of crystal morphology within the bulk was observed by optical microscopy during our measurements. The X-ray diffraction confirmed that the crystalline phase corresponds to orthorhombic Sb_2S_3 (stibnite). The morphology of growing crystals was not dependent on temperature and time in the range of 525–556 K. We found that the crystallization starts predominantly from randomly distributed nuclei (Fig. 5a). The oval crystals were predominately observed (Fig. 5b). The lengths of oval crystals were plotted as time dependence at temperature range of 525–556 K (Fig. 6). Every experimental point and corresponding error was obtained as a mean from at least 10 different crystal objects. Time dependences of crystal's lengths are linear for all measurements. This type of behavior is typical for crystal growth controlled by interface kinetics. The crystal growth rates corresponding to the slope of these dependences are summarized in Table 1. The logarithm of crystal growth u versus reciprocal temperature $1/T$ is shown in Fig. 7. The full lines correspond to the least-square fit of these data. The activation energy of crystal growth $E_G = 295 \pm 3\,\text{kJ mol}^{-1}$ was obtained from the slope of

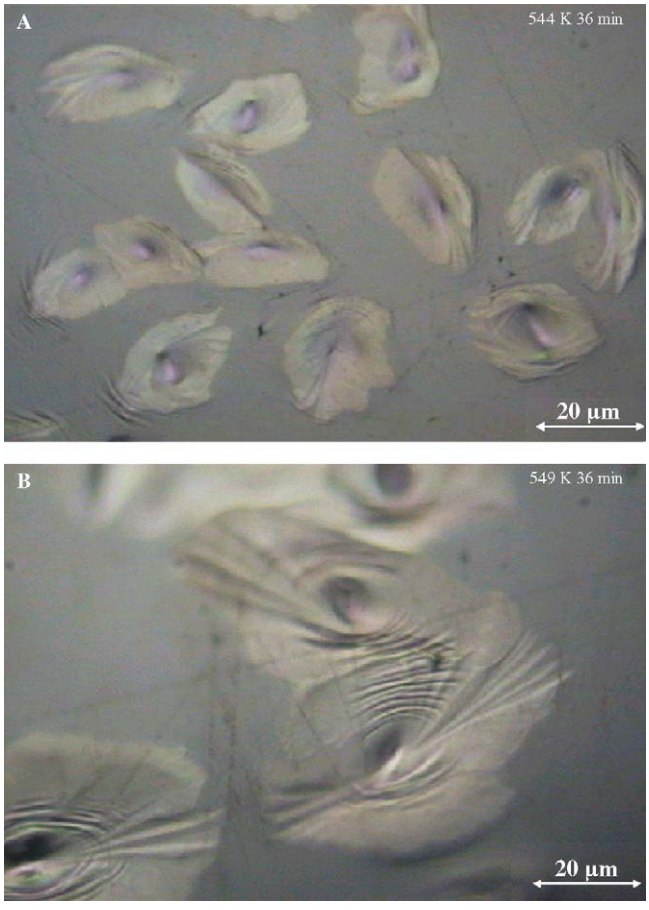

Fig. 5. Randomly distributed crystals of Sb_2S_3 in $(GeS_2)_{0.2}(Sb_2S_3)_{0.8}$ sample (A) and detail of dominant form of crystals in partially crystallized $(GeS_2)_{0.2}(Sb_2S_3)_{0.8}$ sample (B). Photographs were made in reverse light mode of optical microscopy.

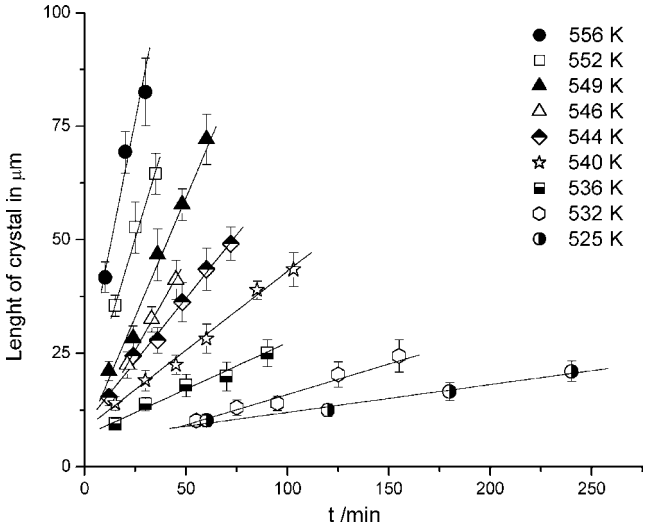

Fig. 6. Time dependence of the length of Sb_2S_3 crystals grown in $(GeS_2)_{0.2}(Sb_2S_3)_{0.8}$ undercooled melt.

Table 1
The crystal growth rate of Sb_2S_3 in $(GeS_2)_{0.2}(Sb_2S_3)_{0.8}$ undercooled melt

Temperature (K)	Growth rate (μm min^{-1})
556	2.25
552	1.48
549	1.05
546	0.79
544	0.56
540	0.35
536	0.20
532	0.13
525	0.06

this plot, premising the Arrhenius behavior (4).

$$u(T) = A_G \times e^{-\frac{E_G}{RT}} \quad (4)$$

where T is the temperature, u is the crystal growth rate, A_G is the pre-exponential factor from growth data and E_G is the apparent activation energy of the crystal growth.

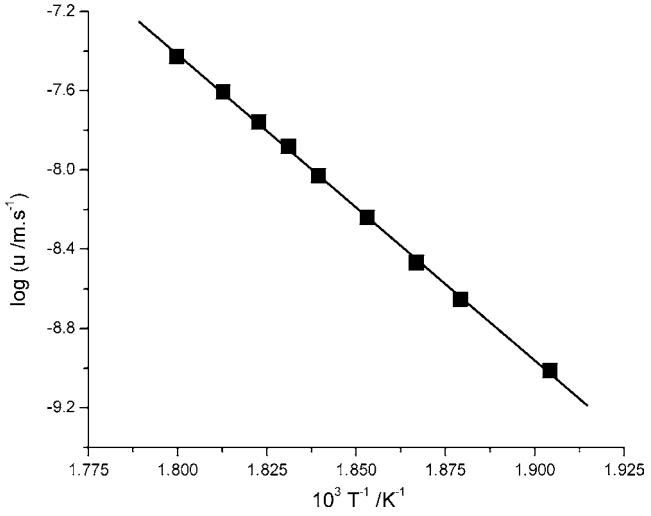

Fig. 7. Arrhenius plot of the crystal growth rate measured by optical microscopy. The line corresponds to the least-square fit of these data.

3.4. X-ray diffraction analysis

Fig. 3 shows typical XRD pattern of amorphous $(GeS_2)_{0.2}(Sb_2S_3)_{0.8}$ glass and fully crystallized material. All diffraction peaks can be assigned to the orthorhombic unit cell of Sb_2S_3 (stibnite). No characteristic peaks of other impurities (GeS, GeS_2) were found. All peaks were assigned by using the JCPDS Card 42-1393.

4. Discussion

The measured heat flow Φ can be described by kinetic equation [11]:

$$\Phi = \Delta H \times A \times \exp\frac{-E}{RT} \times f(\alpha) \quad (5)$$

where ΔH is the crystallization enthalpy, A is the pre-exponential factor and E is the apparent activation energy. The function $f(\alpha)$ is an analytical expression of the kinetic model. One the most widely used kinetic model is Johnson–Mehl–Avrami nucleation-growth model JMA (m) [11]:

$$f(\alpha) = m \times (1-\alpha) \times [-\ln(1-\alpha)]^{1-1/m} \quad (6)$$

where α is the conversion and m is the kinetic exponent which reflects nucleation rate and crystal morphology.

Determination of kinetic model is based on the $z(\alpha)$ and $y(\alpha)$ functions. These functions can be easily obtained by a simple transformation of DSC data. They can be defined under non-isothermal conditions [10]:

$$y(\alpha) = \Phi \times \exp\frac{E}{RT} \quad (7)$$

$$z(\alpha) = \Phi \times T^2 \quad (8)$$

and under isothermal conditions [10]:

$$y(\alpha) = \Phi \quad (9)$$

$$z(\alpha) = \Phi \times t \quad (10)$$

The $z(\alpha)$ and $y(\alpha)$ functions normalized within range $\langle 0; 1\rangle$ under non-isothermal conditions for bulk samples are shown in Fig. 8 (assuming that $E \cong 180\,\text{kJ mol}^{-1}$). The maxima of these dependences were found at α_z (max) = 0.63 ± 0.03 and α_y (max) = 0.43 ± 0.02. Under isothermal conditions are shown $z(\alpha)$ and $y(\alpha)$ normalized functions in Fig. 9. The maxima of these dependences were found at α_z (max) = 0.63 ± 0.01 and α_y (max) = 0.34 ± 0.03. Characteristic value of maximum of $z(\alpha)$ function for JMA(m) kinetic model is 0.632 [10]. The crystallization process of Sb_2S_3 in the bulk form of $(GeS_2)_{0.2}(Sb_2S_3)_{0.8}$ can be described by JMA model under non-isothermal and isothermal conditions. This model has been used in subsequent analysis. The value of parameter m was calculated from equation [12]:

$$m = [1 + \ln(1 - \alpha_y(\text{max}))]^{-1} \quad (11)$$

The value of parameter m is 2.3 ± 0.2 under non-isothermal conditions and 1.7 ± 0.2 under isothermal conditions.

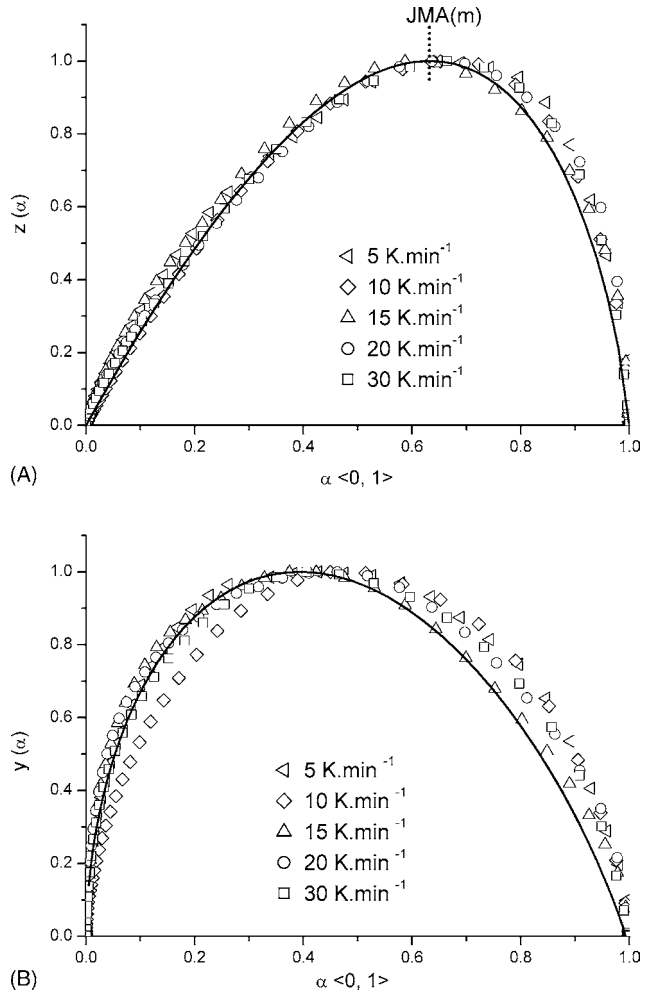

Fig. 8. Normalized $z(\alpha)$ and $y(\alpha)$ function for non-isothermal crystallization of bulk samples of $(GeS_2)_{0.2}(Sb_2S_3)_{0.8}$ undercooled melt. Points correspond to DSC data transformed using Eq. (7) and (8). Solid line is a prediction of JMA equation for $m = 2$.

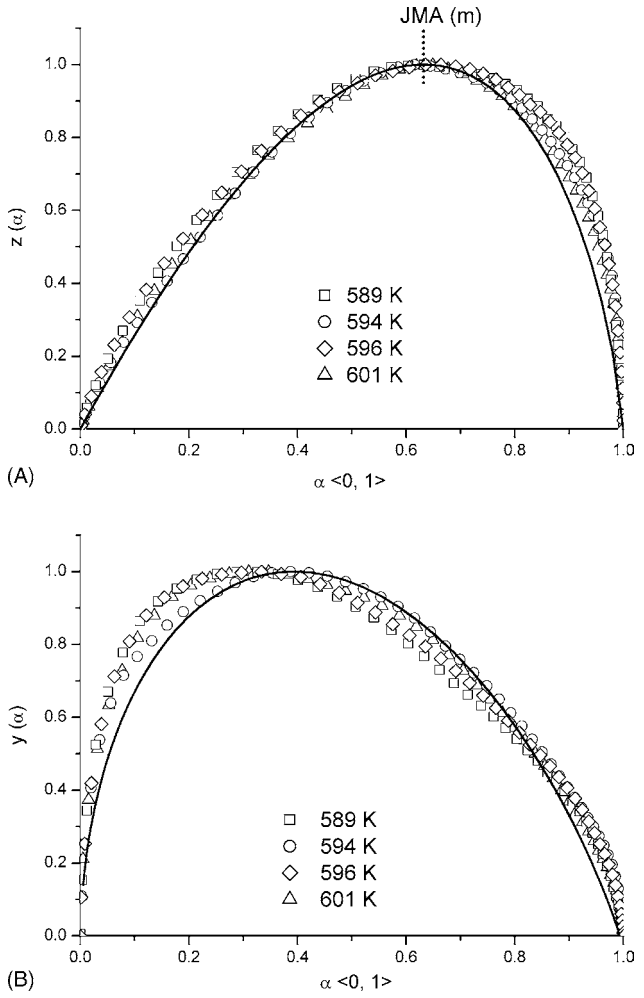

Fig. 9. Normalized $z(\alpha)$ and $y(\alpha)$ function for isothermal crystallization of bulk samples of $(GeS_2)_{0.2}(Sb_2S_3)_{0.8}$ undercooled. Points correspond to DSC data transformed using Eq. (9) and (10). Solid line is a prediction of JMA equation for $m = 2$.

For next kinetic analysis was used Johnson–Mehl–Avrami model with average parameter $m = 2$. Fig. 1 (solid lines) shows non-isothermal DSC curves, calculated by Eq. (5) for $E = 180\,\mathrm{kJ\,mol^{-1}}$, $m = 2$ and $\ln(\mathrm{A/s^{-1}}) = 30.0 \pm 0.1$. In Fig. 2 (solid lines) are shown isothermal DSC curves, calculated by Eq. (5) for $E = 268\,\mathrm{kJ\,mol^{-1}}$, $m = 2$ and $\ln(\mathrm{A/s^{-1}}) = 47.2 \pm 0.1$. The pre-exponential factor was variable and other parameters were constant.

It has been anticipated above that optical measurements reveal features typical for crystal growth controlled by interface kinetics. In this case there are three basic phenomenological models suitable for description of crystal growth in undercooled melt [13]:

- normal growth;
- screw dislocation growth;
- 2D surface nucleated growth.

For molecularly complex liquids can be assumed that reorientation of the molecules or breaking bonds between atoms must precede the incorporation of the molecule into the crystal. This reorientation and bond breaking in fact controls the crystal growth rate u. The usual assumption is that the temperature dependence of the interface process can be described by undercooled melt viscosity η using the Stokes–Einstein relation [13,14]. Jackson et al. [15] has emphasized the importance of a bulk thermodynamic property (as the entropy of fusion ΔS_f) on the crystallization processes and on the nature of crystal–liquid interface in undercooled melts. The operative growth mechanism can be then assessed from the reduced growth rate U_R given by the following equation [13]:

$$U_R = \frac{u \times \eta}{1 - \exp(-\Delta S_f \times \Delta T/RT)} \tag{12}$$

where T is the temperature at which the crystal growth rate u are measured and the viscosity η are extrapolated, ΔT is undercooling with respect to the melting point ($\Delta T = T_m - T$) and ΔS_f is the entropy of fusion of crystalline phase.

The temperature dependence of U_R gives information directly about the growth sites at the interface. In terms of the standard kinetic models, U_R versus ΔT relation for normal growth would be a horizontal line, for screw dislocation growth a line of

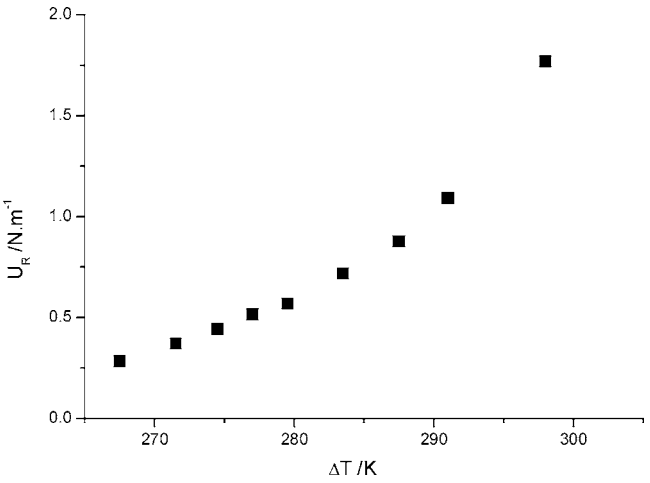

Fig. 10. Reduced growth rate vs. undercooling for crystallization of Sb_2S_3 in undercooled $(GeS_2)_{0.2}(Sb_2S_3)_{0.8}$ melt.

positive slope passing through the origin, and for surface nucleation growth a curve passing thought the origin which would exhibit positive curvature. In our calculations we used the value of entropy of fusion $\Delta S_f = 49.39\,J\,mol^{-1}\,K^{-1}$ and melting point of Sb_2S_3 $T_m = 823\,K$ [16]. Fig. 10 shows the reduced growth rate calculated from experimental growth rate (Table 1) and viscosity data (Fig. 4). The positive curvature of this plot denotes 2D surface nucleated growth. In this case, the growth rate can be expressed as

$$u = \frac{C}{\eta}\exp\left(-\frac{B}{T \times \Delta T}\right) \tag{13}$$

where B and C are constants [13].

Fig. 11 shows the dependence of $\ln(u \times \eta)$ on $(T \times \Delta T)^{-1}$ obtained from our experimental data (points). Solid line corresponds to the least-square fit of these data. It is apparent that the predicted linear dependence is confirmed for crystal growth of Sb_2S_3 in whole temperature range. We obtained parameters $B = (5.3 \pm 0.2) \times 10^6\,K^2$ and $\ln(C/N\,m^{-1}) = 34.1 \pm 1.2$.

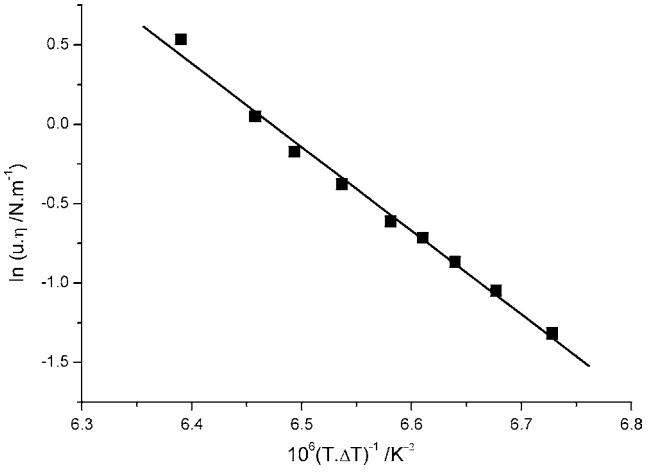

Fig. 11. Plot of logarithm (growth rate x viscosity) vs. $(T \times \Delta T)^{-1}$ for crystallization of Sb_2S_3 in $(GeS_2)_{0.2}(Sb_2S_3)_{0.8}$ undercooled melt. The solid line corresponds to the least-square fit of experimental data.

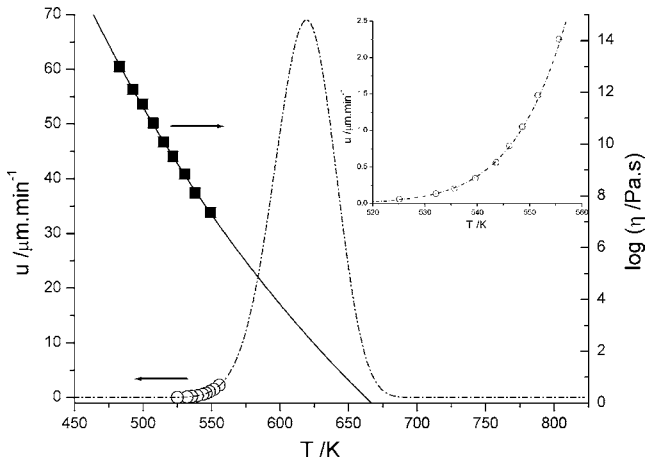

Fig. 12. Temperature dependence of crystal growth rate and viscosity in $(GeS_2)_{0.2}(Sb_2S_3)_{0.8}$ undercooled melt. The dash dotted line corresponds to the calculated data by Eq. (13). Solid line corresponds to extrapolated viscosity data.

In Fig. 12 are plotted the viscosity data ($7 < \log(\eta/Pa\,s) < 13$), the experimental growth rate data (Table 1) and data calculated by using parameters B and C obtained from the $\ln(u \times \eta)$ versus $(T \times \Delta T)^{-1}$ plot (dash dotted line). The optimal conditions for optical observation of Sb_2S_3 crystal growth in $(GeS_2)_{0.2}(Sb_2S_3)_{0.8}$ undercooled melt were for viscosity: $6.9 < \log(\eta/Pa\,s) < 9.2$. The maximum of crystal growth was approximately estimated around 619 K. From Fig. 12 is apparent that the calculated growth rates are relatively in reasonably good agreement with experimental data at a large range of undercooling, although we extrapolate the viscous data.

The observed growth of Sb_2S_3 crystal in undercooled melt of $(GeS_2)_{0.2}(Sb_2S_3)_{0.8}$ composition by optical microscopy takes place at lower temperature than was detected by DSC method under isothermal conditions. We calculated the crystal growth rates will be about 30 $\mu m\,min^{-1}$ at 589 K and about 50 $\mu m\,min^{-1}$ at 601 K. These values of crystal growth for isothermal conditions are too fast and out of observed limits by optical microscopy in our case. The average apparent activation energy for isothermal conditions obtained by isoconversional method is $268 \pm 40\,kJ\,mol^{-1}$ and $180 \pm 4\,kJ\,mol^{-1}$ for non-isothermal conditions. The activation energy calculated by Kissinger method for non-isothermal conditions is $180 \pm 4\,kJ\,mol^{-1}$. The activation energy obtained from optical measurements is $E_G = 295 \pm 3\,kJ\,mol^{-1}$. This value is in the error limits close to activation energy calculated by isoconversional method at isothermal conditions. The activation energies determined by using Kissinger and isoconversional method for non-isothermal conditions are close in the error limits too. The maximum of crystal growth was approximately estimated around 619 K with crystal growth rate 69 $\mu m\,min^{-1}$. The activation energy obtained for viscosity measurements is $E_\eta = 439 \pm 9\,kJ\,mol^{-1}$. Temperature corresponds to viscosity 10^{12} Pa s is 494 K and the temperature glass transition from DSC is about 510 K.

The activation energy of crystal growth represents about 2/3 of the activation energy of viscous flow. A similar result was found for crystallization in $(GeS_2)_{0.3}(Sb_2S_3)_{0.7}$ undercooled

melt [6]. The ratio $E_G/E_\eta \cong 1/2$ was found for crystallization in another chalcogenide systems [7,17].

5. Conclusions

The crystal growth kinetics of Sb_2S_3 in $(GeS_2)_{0.2}(Sb_2S_3)_{0.8}$ undercooled melt has been studied by DSC and optical microscopy. Following conclusions can be formulated.

At the studied range 323–673 K was detected one exothermic peak corresponding to crystallization of Sb_2S_3 (stibnite). The crystallization behavior was described by the Johnson–Mehl–Avrami model with parameter $m = 2$ under non-isothermal and isothermal conditions.

Two-dimensional crystal growth was observed by optical microscopy at the temperature range of $525\,K \leq T \leq 556\,K$. The activation energy of linear crystal growth is $295 \pm 3\,kJ\,mol^{-1}$. Only the orthorhombic Sb_2S_3 crystals were observed.

The interface controlled 2D nucleated growth was determined from the plot of reduced growth rate versus undercooling. The optimal conditions for optical observation of Sb_2S_3 crystal growth are for viscosity: $6.9 < \log(\eta/Pa\,s) < 9.2$. The maximum of crystal growth was approximately estimated around 619 K

Acknowledgments

This work has been supported by the Grant Agency of the Czech Republic under project No. 104/04/0072 and by the Ministry of Education Youth and Sports of the Czech Republic under project LC 523. The authors are indebted to the Joint Laboratory of Solid State Chemistry of the University of Pardubice and the Institute of Macromolecular Chemistry Academy of Sciences of the Czech Republic for providing microscopy facilities.

References

[1] J.D. Desai, C.D. Lokhande, J. Non-Cryst. Solids 181 (1995) 70.
[2] A.M. Salem, M.S. Selim, J. Phys. D: Appl. Phys. 34 (2001) 12.
[3] K.Y. Rajpure, C.D. Likhande, C.H. Bhosale, Mater. Res. Bull. 34 (1999) 1079.
[4] P. Arun, A.G. Vedeshwar, J. Appl. Phys. 79 (1996) 4029.
[5] P. Pustková, D. Švadlák, J. Shánělová, J. Málek, Thermochim. Acta (2006), in press.
[6] J. Málek, D. Švadlák, T. Mitsuhashi, H. Haneda, J. Non-Cryst. Solids, (2006), in press.
[7] J. Shánělová, J. Málek, M.D. Alcalá, J.M. Criado, J. Non-Cryst. Solids 351 (2005) 557.
[8] J. Málek, J. Shánělová, J. Non-Cryst. Solids 243 (1999) 116.
[9] H.E. Kissinger, Anal. Chem. 29 (1957) 1702.
[10] J. Málek, Thermochim. Acta 355 (2000) 239.
[11] J. Šesták, Thermophysical properties of solids, in: Their Measurements and Theoretical Analysis, Elsevier, Amsterdam, 1984.
[12] J. Málek, Thermochim. Acta 138 (1989) 337.
[13] D.R. Uhlmann, in: L.L. Hench, S.W. Freiman (Eds.), Advances in Nucleation and Crystallization in Glasses, American Ceramic Soc., Columbus, 1972.
[14] M.L.F. Nascimento, E.B. Ferreira, E.D. Zanotto, J. Chem. Phys. 121 (2004) 8924.
[15] K.A. Jackson, D.R. Uhlmann, J.D. Hunt, J. Cryst. Growth 1 (1967) 1.
[16] G.K. Johnson, G.N. Papatheodorou, C.E. Johnson, J. Chem. Thermodyn. 13 (1981) 745.
[17] D.W. Henderson, D.G. Ast, J. Non-Cryst. Solids 64 (1984) 43.